RSC Advances

PAPER

View Article Online
View Journal | View Issue

Cite this: *RSC Adv.*, 2017, **7**, 54892

A turn-on fluorescent probe for Cd^{2+} detection in aqueous environments based on an imine functionalized nanoscale metal–organic framework†

Jintong Wang, Tifeng Xia, Xin Zhang, Qi Zhang, Yuanjing Cui, Yu Yang* and Guodong Qian*

Received 10th October 2017
Accepted 26th November 2017

DOI: 10.1039/c7ra11162b

rsc.li/rsc-advances

A novel fluorescent probe was synthesized and explored to detect cadmium ions (Cd^{2+}) based on an imine functionalized metal–organic framework (MOF). The nanoscale MOF probe (~100 nm) displayed a turn-on fluorescence in aqueous environments with the addition of Cd^{2+} which could be ascribed to the interaction between the C=N group and specific metal ions, presenting a low-toxicity, highly selective and sensitive detection method for Cd^{2+} with a detection limit of 0.336 μM (37.8 ppb) and a broad linear range of 0–500 μM, which is promising for application in intracellular sensing and imaging of Cd^{2+}. The probing mechanism was studied and discussed in detail.

Introduction

As one of the extremely toxic and carcinogenic heavy metal ions, the cadmium ion (Cd^{2+}) is widely used in many industrial fields such as the production of metal alloys, batteries, electroplating films and the control rods of atomic/nuclear reactors.[1] However, Cd^{2+} can be easily absorbed and accumulated in the human body *via* food chains with a long biological half-life (about 30 years).[2] Meanwhile, the intake of Cd^{2+} can damage immune systems and increase the incidence of various diseases such as bone pain, pathological fractures, and even kidney cancer and lung cancer.[3] Therefore, the detection of trace Cd^{2+} is critically important.

Up to now, various techniques have been developed for the determination of Cd^{2+} such as atomic absorption spectrometry (AAS),[4] atom emission spectrometry (AES),[5] inductively coupled plasma mass spectrometry (ICP-MS),[6] and synchrotron radiation X-ray spectrometry (XRS).[7] However, normal restrictions of these analytical methods such as sophisticated instruments, complicated sample preparation and time-consuming processes made cheap, remote and on-site detection far from available. It is of vital importance to develop a simple, rapid and sensitive technique for Cd^{2+} detection. Recently, fluorescent sensors have been considered as a promising and compelling candidate, which can sensitively determine Cd^{2+} ions in different environments through the fluorescence intensity changes or wavelength shifts and avoid the complicated time-consuming identification problem.[8] A lot of fluorescent Cd^{2+} probes based on small molecules and polymers have been reported.[9]

Among various fluorescent chemosensors, metal–organic frameworks (MOFs) have aroused tremendous attention during the past decades. By taking advantages of their fascinating luminescent properties, size-adjustable pores, and modifiable recognized sites through postsynthetic modification (PSM),[10] a variety of MOFs have been explored for detecting metal ions including Ag^{+},[11] Al^{3+},[12] Zn^{2+},[13] Cu^{2+},[14] Pb^{2+},[15] Hg^{2+} (ref. 16) *etc.* However, only a few examples of MOF probes capable of detecting Cd^{2+} ions, which were mainly based on luminescent lanthanide MOFs, have been reported up to date.[17] There still remains two challenges in the design of MOF probes for highly selective and sensitive sensing of Cd^{2+} in water samples. One is high accuracy with low deviation of the probe, thus the nanoscale size and stable luminescence are expected. The other is satisfying selectivity and anti-interference ability toward congener elements, for which the sensing mechanism of the Cd^{2+} probe should be based on different binding affinities with various metal ions, instead of selective coordination alone.[8] Thus, a nanoscale MOF whose recognition site has a better affinity with Cd^{2+} may be a possible solution to above problems. Given the good affinity between cadmium ions with nitrogen atoms, we can utilize the imine group as the recognition site.[18] For this purpose, as the corresponding imine linkers are not commercially available and not thermal stable, the PSM strategy is needed to realize the chemical transformation from amine group.[19]

Enlightened by the above thoughts, we herein developed a novel nanoscale fluorescent probe based on imine

State Key Laboratory of Silicon Materials, Cyrus Tang Center for Sensor Materials and Applications, School of Materials Science & Engineering, Zhejiang University, Hangzhou, 310027, P. R. China. E-mail: gdqian@zju.edu.cn; yuyang@zju.edu.cn

† Electronic supplementary information (ESI) available. See DOI: 10.1039/c7ra11162b

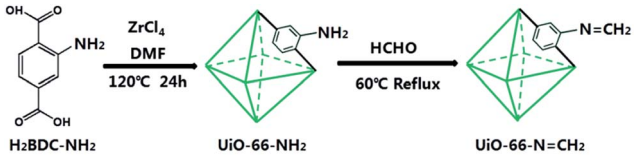

Scheme 1 Schematic illustration of design of MOF-based fluorescent turn-on probe for Cd^{2+}. Postsynthetic modification of **UiO-66-NH_2** to **UiO-66-N=CH_2** *via* condensation reaction.

functionalized MOFs *via* a condensation reaction of **UiO-66-NH_2**. As a promising method, PSM of MOFs has become a new tool for exploiting and expanding the unique properties of MOFs. By transforming amine ($-NH_2$) group of **UiO-66-NH_2** to imine (–N=C) group, we synthesized a 3D porous MOF **UiO-66-N=CH_2** as a novel Cd^{2+} fluorescent probe (Scheme 1). Due to the strong affinity and the coordination between Cd^{2+} with nitrogen atoms in imine group, the MOF probe exhibited fast response, high selectivity, and excellent sensitivity for Cd^{2+} detection in aqueous solution.

Experimental

Chemical reagents

All chemicals and reagents were purchased at least of analytical grade and used without further purification. The standard solutions of metal ions (Cd^{2+}, Na^{+}, Ca^{2+}, Mg^{2+}, Cu^{2+}, Zn^{2+}, Pb^{2+}, Al^{3+} and Fe^{3+}) were prepared from solving their nitrates in deionized water with the concentration of 0.01 M.

Physical measurements

Powder X-ray diffraction (PXRD) patterns were measured within the 2θ range of 3–50° on X'Pert Pro X-ray diffractometer with Cu-K_α radiation ($\lambda = 1.542$ Å) at room temperature. Thermal gravimetric analysis (TGA) were carried out on a Netzsch STA449C system at a heating rate of 10 K min^{-1} from 30 °C to 800 °C under nitrogen atmosphere in the Al_2O_3 crucibles. Fourier transform infrared (FTIR) spectra were recorded within 4000–400 cm^{-1} range on Thermo Fisher Nicolet iS10 spectrometer using KBr pellets. The pellets were prepared by mixing the MOF (about 1 mg) with KBr (about 150 mg). The mixture was then carefully grinded and compressed under the pressure of 10 kPa to form a transparent pellet. ^{1}H NMR spectra were recorded on a Bruker Advance DMX 500 spectrometer using tetramethylsilane (TMS) as an internal standard. The emission and excitation spectra for the samples were recorded by a Hitachi F-4600 fluorescence spectrometer. The morphologies of MOFs were recorded by a S-4800 field-emission scanning electron microscope (FE-SEM). X-ray photoelectron spectroscopy (XPS) was recorded with a Thermo Fisher ESCALAB 250Xi X-ray photoelectron spectrometer with Al Kα X-ray radiation for excitation. The outer luminescent quantum efficiency was determined using an integrating sphere ($BaSO_4$ coating) from Edinburgh FLSP920 fluorescence spectrometer. The quantum yield can be defined as the integrated intensity of the luminescence signal divided by the integrated intensity of the absorption signal.

Synthesis of UiO-66-NH_2

UiO-66-NH_2 was synthesized using a solvothermal method with a modification of previous reports.[20] Anhydrous $ZrCl_4$ (116.6 mg, 0.5 mmol, 1 equiv.), 2-aminoterephthalic acid (108.8 mg, 0.6 mmol, 1.2 equivs), benzoic acid (1.8320 g, 15 mmol, 30 equivs) and deionized water (36.0 μL, 4 equivs) were dissolved in 10 mL *N*,*N*-dimethylformamide (DMF) with ultrasonication for 15 min. Then the homogeneous solution was transferred into a teflon lined autoclave vessel and placed in a 120 °C oven for 24 h. After cooling overnight, the as-synthesized product was rinsed three times with DMF and ethanol to remove unreacted reagents. Then the faint yellow powders were isolated by centrifugation.

Synthesis of UiO-66-N=CH_2

In a typical synthesis, the activated and dried **UiO-66-NH_2** (100 mg, 0.34 mmol of $-NH_2$) was dispersed in one flask (50 mL capacity) with 15 mL of acetone. Six equivalents (per NH_2 functionality, 163 μL) of 40% HCHO (formaldehyde) was added by microlitre pipette. After ultrasonication treated for several minutes, the flask with the mixed solution was heated under reflux and stirring in 60 °C oil bath for 4 h to produce the imine functionalized compound. After repeated centrifugation and rinsing using ethanol for three times, the solid powders was then dried under vacuum at 60 °C overnight to yield the final product, **UiO-66-N=CH_2**.

Luminescent experiments

The photoluminescence properties of **UiO-66-N=CH_2** in different metal cation solutions were studied at 25 °C. In a typical experiment, 2.0 mg powder samples of **UiO-66-N=CH_2** were weighed and introduced into 2.0 mL aqueous solution of $M(NO_3)_n$ ($M^{n+} = Cd^{2+}$, Na^{+}, Ca^{2+}, Mg^{2+}, Cu^{2+}, Zn^{2+}, Pb^{2+}, Al^{3+} and Fe^{3+}) and dispersed ultrasonically to form suspensions for luminescent measurements. Then Cd^{2+} solutions at various concentrations are prepared through dilution of standard solution (0.01 M in deionized water). All the luminescent properties were observed upon excitation at 342 nm.

Digestion and analysis by ^{1}H NMR

^{1}H NMR spectra of MOFs were recorded on a Bruker Advance DMX 500 spectrometer. Approximately 3 mg of **UiO-66-NH_2** and **UiO-66-N=CH_2** were digested with sonication in 600 μL of DMSO-d_6 and 30 μL of DCl.

Cell culture and *in vitro* cytotoxicity assay

Rat pheochromocytoma (PC12) cells were incubated in a humidified incubator (37 °C, 5% CO_2) for three days employing Dulbecco's modified eagle medium (DMEM, Neuronbc) with 10% fetal bovine serum (FBS), and 1% penicillin/streptomycin (P/S, Boster). The toxicity of **UiO-66-N=CH_2** was assessed by MTT assays. The crystals were cultured with PC12 cells for 24 h at five concentrations (5, 20, 50, 80, and 100 μg mL^{-1}) in 96-well assay plates (200 μL total volume per well). The MTT solution (50 μL) was added to each well tested and the plates were

cultured for 4 h. The medium was removed and the blue dye appeared after the addition of DMSO (150 mL). Absorbance values of samples were determined with a microplate reader at $\lambda = 490$ nm. The cell viability was calculated as the ratio of the absorbance of the sample well to that of the control. The results were repeated in triplicate and averaged.

Results and discussion

Crystal synthesis and characterization

As the precursor of the MOF probe in this work, **UiO-66-NH$_2$** was prepared *via* the solvothermal reaction of the **H$_2$BDC-NH$_2$** ligand with $ZrCl_4$ in the solvent DMF (as shown in Scheme 1). **UiO-66-NH$_2$** has attracted intense research interests recently by virtue of the outstanding chemical and thermal stabilities.[21] On account of the unparticipating amine groups of the ligand in coordination to the Zr_6-octahedra $[Zr_6O_4(OH)_4]$ clusters, these free functional groups are thus potentially available for undergoing various chemical modifications. Therefore, the fluorescent probe **UiO-66-N=CH$_2$** was prepared through postsynthetic modification of **UiO-66-NH$_2$** *via* aldehyde-amine condensation reaction. In a typical synthesis (Scheme 1), freshly activated **UiO-66-NH$_2$** was treated by formaldehyde under reflux in acetone for 4 h to produce the corresponding imine compound **UiO-66-N=CH$_2$**.

The phase purity of **UiO-66-NH$_2$** and **UiO-66-N=CH$_2$** were confirmed by overlapping powder X-ray diffraction (PXRD) patterns of simulated and as-synthesized samples. As shown in Fig. 1a, the PXRD patterns of as-synthesized **UiO-66-NH$_2$** and **UiO-66-N=CH$_2$** matched well with simulated PXRD pattern of UiO-66, which can be featured by two peaks at 7.4° and 8.5°, representing the crystal plane (111) and (200) respectively.[22]

Furthermore, to confirm the thermal stability and structural integrity of two MOFs at elevated temperatures, samples were examined by TGA (Fig. S1†). The TGA curves revealed that **UiO-66-NH$_2$** and the ethanol-treated **UiO-66-N=CH$_2$** will lose entrapped solvent molecules at 100 °C and 80 °C, respectively. Similarly, both two MOFs showed high thermal stability with decomposition temperatures up to 400 °C. The permanent porosity of the prepared **UiO-66-NH$_2$** was determined by N_2 adsorption–desorption isotherm after guest removal, exhibiting a BET surface area of 934.4 $m^2\ g^{-1}$. The reactive nature of the free $-NH_2$ groups and the permanent porosity of **UiO-66-NH$_2$** are potentially available for conducting various modifications. And after postsynthetic modification, the synthesized **UiO-66-N=CH$_2$** displayed analogous N_2 adsorption–desorption behaviour (Fig. S2†), which showed a decreased BET surface area of 689.3 $m^2\ g^{-1}$ as expected, indicating that **UiO-66-N=CH$_2$** still maintains its permanent pores.

Field-emission scanning electron microscopy (FE-SEM) images (Fig. 2) were taken to reveal the morphology of the synthesized **UiO-66-NH$_2$**. In this work, 30 equivalents benzonic acid were employed as the modulator, and the as-synthesized faint yellow powders displayed perfect octahedral morphology with particle sizes about 100 nm. It is also worth mentioning here that a smaller particle size is not only conducive to guest molecules transfer within **UiO-66-NH$_2$** crystals, but also critical

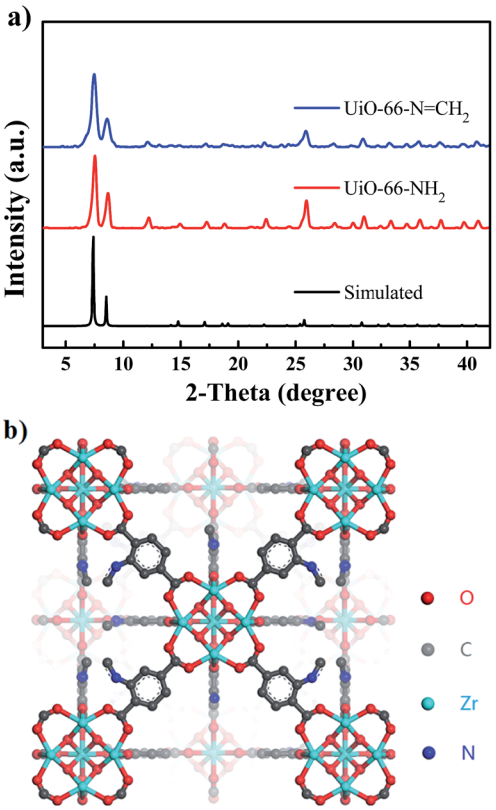

Fig. 1 Synthesis and characterization of UiO-66-NH$_2$ and UiO-66-N=CH$_2$. (a) PXRD patterns of the simulated UiO-66-NH$_2$ (black), as-synthesized UiO-66-NH$_2$ (red) and UiO-66-N=CH$_2$ (blue). (b) Structure depiction of UiO-66-N=CH$_2$.

to be developed as a fluorescent probe. Additionally, these materials were characterized by FTIR spectroscopy (Fig. S3†). The FTIR spectra of **UiO-66-NH$_2$** show two peaks at 3345 and 3456 cm^{-1} due to the existence of the symmetric and asymmetric stretching of primary amines, which demonstrates that the amino groups are free for interaction in these structures. But FTIR spectroscopy is less revealing with the framework $-NH_2$ stretching bands dominating, thus obscuring any imine (C=N) and –OH stretches. In addition, unambiguous characterization was provided by liquid ^{1}H NMR analysis (Fig. S4†). Samples of **UiO-66-NH$_2$** and **UiO-66-N=CH$_2$** were digested and dissolved in dilute DCl/D_2O/DMSO-d_6 solution and then analyzed by ^{1}H NMR spectroscopy, which confirmed the formation of the imine compound by the appearance of new

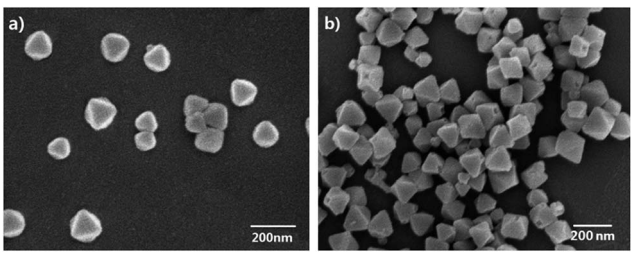

Fig. 2 FE-SEM images of UiO-66-NH$_2$ and UiO-66-N=CH$_2$.

signals (7.84–7.85 ppm, d, (H)C=N) (Fig. S4d†). It is obvious that the aromatic signals of the amine (7 ppm, d, 1H; 7.34 ppm, s, 1H; 7.77 ppm, d, 1H) (Fig. S4c and d†) does not completely disappear, indicating not full conversion to the imine form.

Photoluminescence properties

The photoluminescent (PL) properties of the MOF probe obtained after successful PSM was first investigated at room temperature. The excitation and emission spectra of **UiO-66-N=CH$_2$** are shown in Fig. 3a. It is clearly observed that the excitation spectra collected in the wavelength range of 200–400 nm are dominated by a broad absorption band in ultraviolet region centered at about 342 nm. The excitation spectra suggest that the probe can absorb the energy of ultraviolet light efficiently. Upon 342 nm radiation in water, crystals of **UiO-66-N=CH$_2$** exhibits a broad peak centered at 468 nm.

To examine the potential of **UiO-66-N=CH$_2$** as a fluorescent probe for metal ions in aqueous environment, the luminescent stability of the sample in aqueous solution has been investigated. During storage in water for 2 weeks, the luminescence intensity of the **UiO-66-N=CH$_2$** suspension shows no significant change (Fig. S5a†), implying the excellent stability of fluorescence in water. Moreover, **UiO-66-N=CH$_2$** also exhibits good pH-independent fluorescence in the pH range of 4–10 (Fig. S5b†), which indicates that the influence of slight fluctuation of pH value on the fluorescent intensity and sensing properties may be neglected.

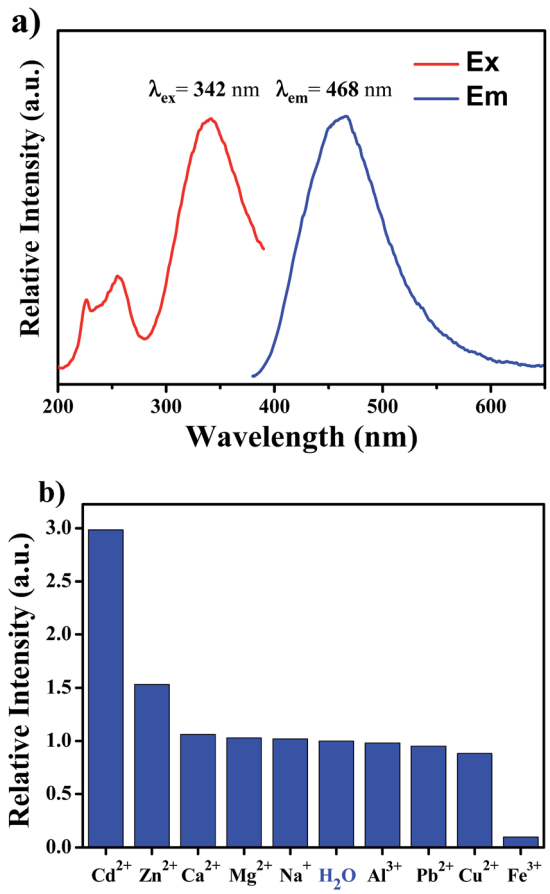

Fig. 3 (a) Excitation (red line) and emission (blue line) spectra of UiO-66-N=CH$_2$; (b) the intensities at 468 nm for UiO-66-N=CH$_2$ dispersed in various metal ion aqueous solutions (500 μM) upon excitation at 342 nm.

Sensing of Cd^{2+}

High selectivity over competing species is of vital importance for a fluorescent probe. For verifying the sensing selectivity of **UiO-66-N=CH$_2$** of metal ions, the suspension-state luminescent experiments are performed. Different kinds of metal ions (Cd^{2+}, Na^{+}, Ca^{2+}, Mg^{2+}, Cu^{2+}, Zn^{2+}, Pb^{2+}, Al^{3+} and Fe^{3+}) have been introduced into the system of **UiO-66-N=CH$_2$**, forming 500 μM aqueous suspensions after ultrasonication treatment for 1 minute. The luminescent spectra showed that the PL intensity of **UiO-66-N=CH$_2$** suspension is largely dependent on the interacted metal ion. As can be seen in Fig. 3b and S6,† only Fe^{3+} causes the quenching effect on the luminescence intensity of **UiO-66-N=CH$_2$**. The addition of Cd^{2+} ion enhanced the luminescence intensity most remarkably by about 3-fold as much as that of the original one, which is the most drastic enhancement effect among all the tested ions. Meanwhile, the luminescence intensity of **UiO-66-N=CH$_2$** showed small increase by Zn^{2+}, which is an important disruptor. The rest of other metal ions had a negligible effect on the luminescence of **UiO-66-N=CH$_2$**. The above results prove that **UiO-66-N=CH$_2$** has a high selectivity for the specific recognition of Cd^{2+} in aqueous environment.

In Fig. 4, we measured the luminescence responses of **UiO-66-N=CH$_2$** (1 mg mL^{-1}) immersed in Cd^{2+} aqueous solutions with different concentrations. It is obvious that the luminescence intensity of **UiO-66-N=CH$_2$** incorporated with Cd^{2+} displays a strong dependence on the concentration of Cd^{2+} ion. As can be seen in Fig. 4a, the emission intensity of **UiO-66-N=CH$_2$** increases gradually with the increase of Cd^{2+} concentration from 0 to 500 μM. Quantitatively, the enhancing effect can be analyzed by the Stern–Volmer equation:

$$I/I_0 = 1 + K_{SV}[Cd^{2+}] \quad (1)$$

where I_0 and I are the luminescence intensity of the suspension at 468 nm in the absence and presence of Cd^{2+}, respectively, K_{SV} represents the Stern–Volmer quenching constant, and $[Cd^{2+}]$ is the concentration of Cd^{2+}. There is a good linear relationship (correlation coefficient R^2 = 0.999) between I/I_0 and $[Cd^{2+}]$ in a wide concentration range (Fig. 4b), indicating that the enhancing effect of Cd^{2+} on the luminescence of **UiO-66-N=CH$_2$** agrees the Stern–Volmer mode well. The K_{SV} value is calculated to be 3.81 × 10^3 M^{-1}, which reveals a strong enhancing effect on the **UiO-66-N=CH$_2$** luminescence. From the slope of the fitting line (slope) and the standard deviation (SD) for eleven replicating fluorescence measurements of blank solutions (Fig. S7†), the detection limit (3SD/slope) of **UiO-66-N=CH$_2$** towards Cd^{2+} was calculated to be 0.336 μM (37.8 ppb).

To evaluate the cytotoxicity of **UiO-66-N=CH$_2$**, rat pheochromocytoma (PC12) cells were selected for *in vitro* studies using the MTT assay, considering the wide use of PC12 cells in

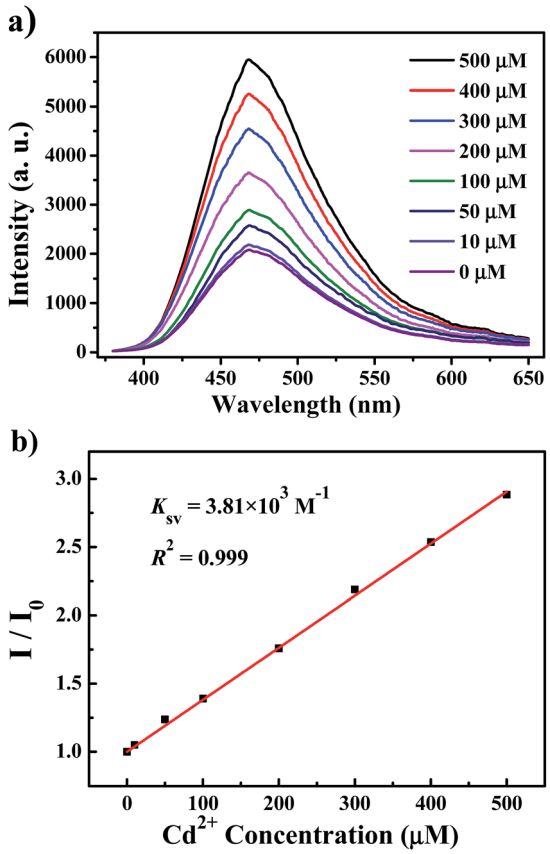

Fig. 4 (a) The luminescent emission spectra (excited at 342 nm) of UiO-66-N=CH_2 (1 mg mL^{-1}) in Cd^{2+} solutions with different concentrations. (b) Stern–Volmer plots of I/I_0 *versus* Cd^{2+} concentration and the fitting line in water ($R^2 = 0.999$; $K_{SV} = 3.81 \times 10^3\ M^{-1}$).

assessing the cytotoxicity of nanomaterials.[23] The MTT assay was carried out by incubating PC12 cells with **UiO-66-N=CH_2** for 24 h at various concentrations ranging from 5 to 100 μg mL^{-1}. As revealed in Fig. S8,† the cell viability decreased slightly with the increase of the **UiO-66-N=CH_2** concentration, but the cell viability was still higher than 80% even at 100 μg mL^{-1}, meaning that **UiO-66-N=CH_2** was a biocompatible probe with negligible cytotoxicity.

The enhancing effect on luminescence of **UiO-66-N=CH_2** by Cd^{2+} ions can be ascribed to the interaction between Cd^{2+} ions and the C=N group within **UiO-66-N=CH_2** which facilitates the efficiency of deactivation from excited state to ground state. To explore the possible mechanism for such luminescence enhancement by Cd^{2+}, N 1s and Cd 3d X-ray photoelectron spectroscopy (XPS) studies were carried out on probe and Cd^{2+}-incorporated probe. The N 1s peak from free imine nitrogen atoms at 399.5 eV in H_2O is shifted to 400.2 eV on the addition of Cd^{2+} (Fig. 5), indicating the weak binding between Cd^{2+} and imine nitrogen atoms in Cd^{2+}-incorporated probe. Such coordination binding of Cd^{2+} with the imine group of the ligand can reduce non-radiative transition and decrease energy loss, thus resulting in a ligand-centered charge transfer which may lead to the enhancing effect. The peak at 413.2 eV in the N 1s XPS spectra for Cd^{2+}-incorporated probe is attributed to Cd 3d, as for

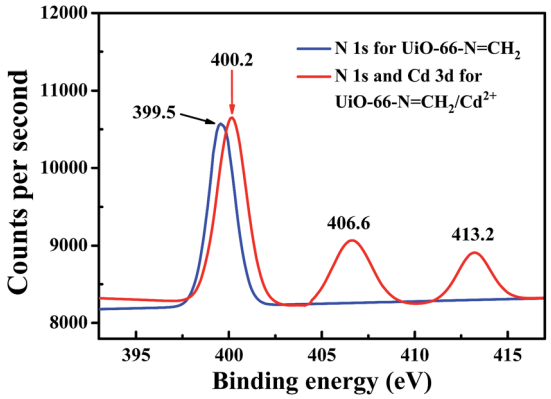

Fig. 5 XPS spectra of the original probe (blue) and Cd^{2+}-incorporated probe (red) activated in 10 mM aqueous solution of $Cd(NO_3)_2$.

the other peak at 406.6 eV, it should be ascribed to the signal of NO_3^- counterions.[24] As a control experiment, we also investigated the fluorescent response of **UiO-66-NH_2** toward Cd^{2+}. After immersing into the Cd^{2+} solution (500 μM), no obvious change was found from the luminescence intensity of **UiO-66-NH_2**, indicating the important role of the C=N group in Cd^{2+} sensing.

As a luminescent probe, **UiO-66-N=CH_2** is not only highly selective and sensitive for Cd^{2+} detection, but also water-stable and nano-scale, which enable the probe to be applicable for Cd^{2+} sensing in aqueous and intracellular environments.

Conclusions

In summary, a novel turn-on fluorescent probe based on imine functionalized nano MOF for Cd^{2+} detection has been synthesized through a post-synthetic approach. The MOF probe displayed high sensitivity (detection limit, 0.336 μM), broad linear range (0–500 μM) and excellent selectivity toward Cd^{2+} over other relevant metal ions. Moreover, it is water-stable, nano-scale and low-toxic. All these indicate the potential of **UiO-66-N=CH_2** for intracellular Cd^{2+} turn-on sensing and imaging.

Conflicts of interest

There are no conflicts to declare.

Acknowledgements

The authors gratefully acknowledge the financial support for this work from the National Natural Science Foundation of China (Nos. 51372221, 51472217, 51432001, 51632008, and U1609219), and Zhejiang Provincial Natural Science Foundation of China (No. LZ15E020001).

Notes and references

1 (*a*) A. M. S. Mendes, G. P. Duda, C. W. A. Nascimento and M. O. Silva, *Sci. Agric.*, 2006, **63**, 328; (*b*) M. Lenzen, *Energy Convers. Manage.*, 2008, **49**, 2178.

2 (*a*) L. T. Lu, I. C. Chang, T. Y. Hsiao, Y. H. Yu and H. W. Ma, *Environ. Sci. Pollut. Res.*, 2007, **14**, 49; (*b*) M. Zhang, Y. Liu and B. Ye, *Analyst*, 2011, **137**, 601.

3 (*a*) Y. Itokawa, K. Nishino, M. Takashima, T. Nakata, H. Katio, E. Okamoto, K. Daijo and J. Kawamura, *Environ. Res.*, 1978, **15**, 206; (*b*) S. Satarug, J. R. Baker, S. Urbenjapol, M. Haswell-Elkins, P. E. Reilly, D. J. Williams and M. R. Moore, *Toxicol. Lett.*, 2003, **137**, 65.

4 A. N. Anthemidis, *Microchim. Acta*, 2008, **160**, 455.

5 A. C. Davis, C. P. Calloway Jr and B. T. Jones, *Talanta*, 2007, **71**, 1144.

6 E. A. Hutton, J. T. van Elteren, B. Ogorevc and M. R. Smyth, *Talanta*, 2004, **63**, 849.

7 E. Marguí, I. Queralt and M. Hidalgo, *J. Anal. At. Spectrom.*, 2013, **28**, 266.

8 (*a*) T. Xia, T. Song, G. Zhang, Y. Cui, Y. Yang, Z. Wang and G. Qian, *Chem.–Eur. J.*, 2016, **22**, 18429; (*b*) J. Yin, T. Wu, J. Song, Q. Zhang, S. Liu, R. Xu and H. Duan, *Chem. Mater.*, 2011, **23**, 4756.

9 (*a*) T. Cheng, T. Wang, W. Zhu, X. Chen, Y. Yang, Y. Xu and X. Qian, *Org. Lett.*, 2011, **13**, 3656; (*b*) Z. Liu, C. Zhang, W. He, Z. Yang, X. Gao and Z. Guo, *Chem. Commun.*, 2010, **46**, 6138; (*c*) L. Xu, M. He, H. Yang and X. Qian, *Dalton Trans.*, 2013, **42**, 8218; (*d*) H. Un, C. Huang, J. Huang, C. Huang, T. Jia and L. Xu, *Chem.–Asian J.*, 2014, **9**, 3397; (*e*) Y. Ren, N. Wu, J. Huang, Z. Xu, D. Sun, C. Wang and L. Xu, *Chem. Commun.*, 2015, **51**, 15153; (*f*) Z. Xu, G. Li, Y. Ren, H. Huang, X. Wen, Q. Xu, X. Fan, Z. Huang, J. Huang and L. Xu, *Dalton Trans.*, 2016, **45**, 12087; (*g*) C. Huang, L. Xu, J. Zhu, Y. Wang, B. Sun, X. Li and H. Yang, *J. Am. Chem. Soc.*, 2017, **139**, 9459.

10 (*a*) Y. Cui, Y. Yue, G. Qian and B. Chen, *Chem. Rev.*, 2012, **112**, 1126; (*b*) Y. Cui, B. Li, H. He, W. Zhou, B. Chen and G. Qian, *Acc. Chem. Res.*, 2016, **392**, 86.

11 J. Hao and B. Yan, *J. Mater. Chem. A*, 2014, **2**, 18018.

12 X. Shi, H. Wang, T. Han, X. Feng, B. Tong, J. Shi, J. Zhi and Y. Dong, *J. Mater. Chem.*, 2012, **22**, 19296.

13 Q. Tang, S. Liu, Y. Liu, J. Miao, S. Li, L. Zhang, Z. Shi and Z. Zheng, *Inorg. Chem.*, 2013, **52**, 2799.

14 B. Chen, L. Wang, Y. Xiao, F. R. Fronczek, M. Xue, Y. Cui and G. Qian, *Angew. Chem., Int. Ed.*, 2009, **121**, 508.

15 L. Li, Q. Chen, Z. Niu, X. Zhou, T. Yang and W. Huang, *J. Mater. Chem. C*, 2016, **4**, 1900.

16 X. Xu and B. Yan, *J. Mater. Chem. C*, 2016, **4**, 1543.

17 (*a*) J. Hao and B. Yan, *Chem. Commun.*, 2015, **51**, 7737; (*b*) C. Liu and B. Yan, *J. Colloid Interface Sci.*, 2015, **459**, 206; (*c*) X. Xu and B. Yan, *Sens. Actuators, B*, 2016, **222**, 347.

18 (*a*) H. Zhu, J. Fan, B. Wang and X. Peng, *Chem. Soc. Rev.*, 2015, **44**, 4337; (*b*) H. J. Jung, N. Singh and D. O. Jang, *Tetrahedron Lett.*, 2008, **49**, 2960.

19 S. M. Cohen, *Chem. Rev.*, 2012, **112**, 970.

20 (*a*) M. Kandiah, M. H. Nilsen, S. Usseglio, S. Jakobsen, U. Olsbye, M. Tilset, C. Larabi, E. A. Quadrelli, F. Bonino and K. P. Lillerud, *Chem. Mater.*, 2010, **22**, 6632; (*b*) A. Schaate, P. Roy, A. Godt, J. Lippke, F. Waltz, M. Wiebcke and P. Behrens, *Chem.–Eur. J.*, 2011, **17**, 6643.

21 (*a*) G. W. Peterson, J. J. Mahle, J. B. Decoste, W. O. Gordon and J. A. Rossin, *Angew. Chem., Int. Ed.*, 2016, **128**, 6343; (*b*) L. Shen, W. Wu, R. Liang, R. Lin and L. Wu, *Nanoscale*, 2013, **5**, 9374; (*c*) S. S. Nagarkar, T. Saha, A. V. Desai, P. Talukdar and S. K. Ghosh, *Sci. Rep.*, 2014, **4**, 7053.

22 (*a*) X. Zhang, Q. Hu, T. Xia, J. Zhang, Y. Yang, Y. Cui, B. Chen and G. Qian, *ACS Appl. Mater. Interfaces*, 2016, **8**, 32259; (*b*) J. H. Cavka, S. Jakobsen, U. Olsbye, N. Guillou, C. Lamberti, S. Bordiga and K. P. Lillerud, *J. Am. Chem. Soc.*, 2008, **130**, 13850.

23 K. Jiang, L. Zhang, Q. Hu, D. Zhao, T. Xia, W. Lin, Y. Yang, Y. Cui, Y. Yang and G. Qian, *J. Mater. Chem. B*, 2016, **4**, 6398.

24 S. Liu, Z. Xiang, Z. Hu, X. Zheng and D. Cao, *J. Mater. Chem.*, 2011, **21**, 6649.